Calorimetric Characterization of Parallel-Stranded DNA: Stability, Conformational Flexibility, and Ion Binding

Dionisios Rentzeperis,[†] Karsten Rippe,[‡] Thomas M. Jovin,[‡] and Luis A. Marky*,[†]

Contribution from the Department of Chemistry, New York University, New York, New York 10003, and Department of Molecular Biology, Max Planck Institute for Biophysical Chemistry, Postfach 2841, D-W-3400 Göttingen, FRG. *Received December 3, 1991*

Abstract: Parallel-stranded DNA is a novel double-stranded, helical form of DNA. Its secondary structure is established by *reverse* Watson–Crick base pairing between the bases of the complementary strands, forming two equivalent grooves. A combination of differential scanning calorimetry and temperature-dependent UV spectroscopy techniques have been employed to characterize the stability, conformational flexibility, and counterion binding of two sets of 25-mer deoxyoligonucleotide duplexes containing either exclusively dA·dT base pairs or substitutions with four dG·dC base pairs. These form either parallel-stranded (ps-D1·D2 and ps-D5·D6) or antiparallel-stranded (aps-D1·D3 and aps-D5·D7) duplexes. All four duplexes show two-state transition behavior with similar values for the thermodynamic release of counterions, indicating that the charge densities are similar. The parallel duplexes melt with both lower T_m values (by 17 and 34 °C, ±0.7 °C) and lower transition enthalpies (34 and 51 kcal·mol^{-1}, ±3 kcal mol^{-1}) than the corresponding antiparallel reference duplexes. These unfavorable differential free energy terms are enthalpically driven, reflecting a reduction in base-stacking interactions and in hydrogen bonding for the case of the duplexes containing dG·dC base pairs. Substitution of four dA·dT base pairs of the ps-D1·D2 duplex for four dG·dC base pairs to create the ps-D5·D6 duplex results in a destabilization of 11.9 °C that is entropically driven. The same substitution in the aps duplexes results in a stabilization of 4.9 °C that is enthalpically driven.

Introduction

A recent addition to the well-known families of DNA conformations[1] is that of parallel-stranded DNA (ps-DNA).[2-5] In this novel structure the complementary strands are in a parallel orientation, held together by *reverse* Watson–Crick base pairs, forming a double helix with two equivalent grooves[4] (for a review, see ref 5). We report the first calorimetric investigation of the helix–coil transition of two parallel 25-mer duplexes (Figure 1), which have been characterized previously by optical means.[2-8] Using a combination of differential scanning calorimetry and temperature-dependent UV spectroscopy techniques, we characterized the thermodynamic nature of the molecular forces, conformational flexibility, and interaction with counterions. The favorable free energy change resulting from the formation of a duplex in the parallel orientation is due to the partial compensation of a favorable enthalpy and an unfavorable entropy. The destabilization of the parallel duplexes relative to the antiparallel duplexes of identical sequences is enthalpic in origin, reflecting a reduction in base-stacking interactions and in hydrogen bonding for the case of the dG·dC base pairs.[7] All duplexes melt in two-state transitions with similar values for the thermodynamic release of counterions, indicating similar charge density parameters.[9]

Experimental Section

Materials. The six oligomeric strands (Figure 1) used in this study were synthesized using standard phosphoramidite chemistry[10] on an Applied Biosystems Model 391 PCR-Mate automated synthesizer. Purification was by HPLC anionic-exchange chromatography with a Du Pont Zorbax Bio column followed by desalting with a Sephadex G-10 exclusion chromatography column. The concentration of each oligomer in solution was determined spectrophotometrically at 260 nm and 80 °C in H_2O, using the following extinction coefficients in $\mu M^{-1}\cdot cm^{-1}$: D1, ϵ = 0.282; D2, ϵ = 0.250; D3, ϵ = 0.250; D5, ϵ = 0.283; D6, ϵ = 0.245; and D7, ϵ = 0.240. These extinction coefficients[11] were obtained by extrapolation to high temperatures of the calculated extinctions at 25 °C using the melting curves of the single strands in H_2O. The buffer solution consisted of 10 mM sodium cacodylate and 0.1 mM Na_2EDTA, at pH 7.0, adjusted to the desired ionic strength with NaCl.

High-Sensitivity Differential Scanning Calorimetry (DSC). Heat capacity vs temperature profiles were obtained with a Microcal MC-2 differential scanning calorimeter. The instrument was calibrated with a standard electrical pulse. Typically an oligomer solution with a concentration of ~150 μM (in strands) vs buffer was scanned from 10 to 80 °C at a heating rate of 45 °C/h. The sample scan was corrected by subtracting a buffer vs buffer scan and normalized by the heating rate. The area under the curve, divided by the number of moles, is equal to the transition enthalpy (ΔH_{cal}). These enthalpies correspond to the total molar heat uptake for the transition of a duplex in a particular conformation at low temperatures to single strands at high temperatures. Shape analysis of these curves yielded the two-state enthalpies (ΔH_{vH}). Direct comparison of ΔH_{vH} with ΔH_{cal} allows us to predict the nature of the transition. In addition, transition entropies and free energies were obtained directly from integration of the $\Delta C_p/T$ vs T curves and the Gibbs equation, respectively.

Temperature-Dependent UV Spectroscopy. Absorbance vs temperature profiles (melting curves) for the oligomeric duplexes as a function of strand concentration and salt concentrations were measured at 260 nm with a thermoelectrically controlled Perkin-Elmer 552 spectrophotometer interfaced to a PC-XT computer for acquisition and analysis of experimental data. The temperature was scanned at a heating rate of 1 °C/min. These melting curves allow us to measure the transition temperatures, T_m, which are the midpoints of the order–disorder transition of these oligomers, as well as the relevant thermodynamic parameters. Transition enthalpies were calculated from shape analysis of the curves and from the T_m–concentration dependence curves using standard procedures reported elsewhere[12,13] and correspond to a two-state approxi-

* To whom correspondence should be addressed.
† New York University.
‡ Max Planck Institute.

(1) Saenger, W. *Principles of Nucleic Acid Structure*; Springer-Verlag: New York, 1984.
(2) van de Sande, J. H.; Ramsing, N. B.; Germann, M. W.; Elhorst, W.; Kalisch, B. W.; Kitzing, E. V.; Pon, R. T.; Clegg, R. C.; Jovin, T. M. *Science* **1988**, *241*, 551.
(3) Ramsing, N. B.; Jovin, T. M. *Nucleic Acids Res.* **1988**, *16*, 6659.
(4) Rippe, K.; Ramsing, N. B.; Jovin, T. M. *Biochemistry* **1989**, *28*, 9536.
(5) Jovin, T. M.; Rippe, K.; Ramsing, N. B.; Klement, R.; Elhorst, W.; Vojtisková, M. In *Structure & Methods, Vol. 3: DNA & RNA*; Sarma, R. H., Sarma, M. H., Eds.; **1991**; p 155.
(6) Ramsing, N. B.; Rippe, K.; Jovin, T. M. *Biochemistry* **1989**, *28*, 9528.
(7) Rippe, K.; Ramsing, N. B.; Klement, R.; Jovin, T. M. *J. Biomol. Struct. Dyn.* **1990**, *7*, 1199.
(8) Rippe, K.; Jovin, T. M. DNA Structures, part A: Synthesis and physical analysis of DNA. *Methods Enzymol.*, in press.
(9) Record, M. T., Jr.; Anderson, C. F.; Lohman, T. M. *Q. Rev. Biophys.* **1978**, *11*, 103.
(10) Caruthers, M. H. In *Chemical and Enzymatic Synthesis of Gene Fragments*; Gassen, H. G., Lang, A., Eds.; Verlag Chemie: Weinheim, FRG, 1982; pp 71–79.
(11) Cantor, C. R.; Warshaw, M. M.; Shapiro, H. *Biopolymers* **1970**, *9*, 1059.
(12) Marky, L. A.; Canuel, L.; Jones, R. A.; Breslauer, K. J. *Biophys. Chem.* **1981**, *13*, 141.
(13) Marky, L. A.; Breslauer, K. J. *Biopolymers* **1987**, *26*, 1601.

0002-7863/92/1514-5926$03.00/0

Table I. Thermodynamic Parameters of Duplex Formation at 5 °C

	calorimetry[a]					UV spectroscopy[b]			
duplex	T_m (°C)	$\Delta H°_{vH}$ (kcal·mol^{-1})	$\Delta H°_{cal}$ (kcal·mol^{-1})	$\Delta G°$ (kcal·mol^{-1})	$T\Delta S°$ (kcal·mol^{-1})	T_m (°C)	$\Delta H°_{shape}$ (kcal·mol^{-1})	$\Delta H°_{vH}$ (kcal·mol^{-1})	Δn_{Na^+} (mol of Na^+/mol of P_i)
ps-D1·D2	37.0	−121	−117	−13	−104	32.2 (29.0)	−128 (−110)	−132	0.137
aps-D1·D3	54.1	−150	−151	−24	−127	50.0 (46.4)	−152 (−160)	−167	0.118
ps-D5·D6	25.1	−113	−116	−10	−106	19.9 (15.7)	−103 (−89)	−120	0.106
aps-D5·D7	59.0	−177	−167	−28	−139	56.7 (52.9)	−145 (−136)	−186	0.135

[a] The calorimetric T_m values at the strand concentration of the DSC experiments (see Figure 2), ΔH_{vH} from the shape of the DSC curves, and $\Delta H°_{cal}$ from the area of the DSC curves. The $\Delta H°_{cal}$ values are within ±3% and the ΔH_{vH} values are within ±10% experimental error. $\Delta S°$ was calculated by integrating $\Delta C_p/T$ vs T curves from DSC, and $\Delta G°$ was calculated from the Gibbs equation at 5 °C. The $T\Delta S°$ values are within 5% experimental error. [b] Spectroscopic transition enthalpies were obtained as follows: $\Delta H°_{shape}$ from the shape of UV melting curves and ΔH_{vH} from the plot of $1/T_m$ vs ln ($C_T/4$). The van't Hoff enthalpies are within ±10% experimental error. The given T_m values correspond to a strand concentration of 2 μM. The values in parentheses are taken from refs 4, 7, and 8.

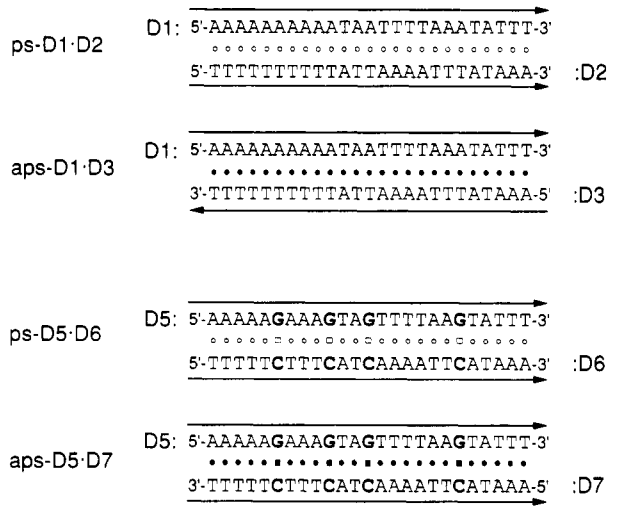

Figure 1. Sequences of synthetic oligonucleotides and their duplexes. The Watson–Crick base pairs of the antiparallel-stranded duplexes are denoted by the closed symbols, and the *reverse* Watson–Crick base pairs of the parallel-stranded duplexes are denoted by the open symbols. Nomenclature as in refs 4, 7, and 8.

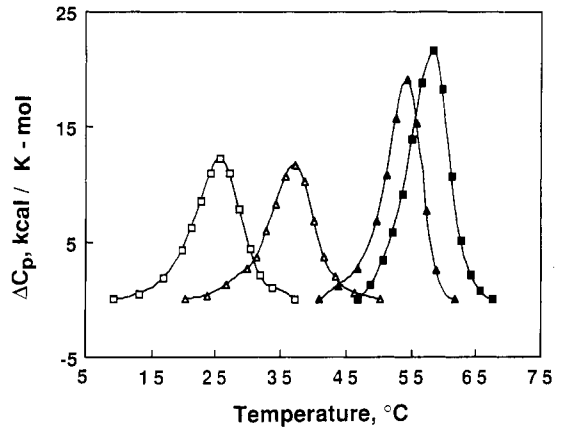

Figure 2. Differential scanning calorimetry curves for each oligomer duplex in 10 mM sodium cacodylate buffer containing 0.1 mM Na_2EDTA and 0.1 M NaCl at pH 7 and indicated total strand concentration: ps-D1·D2, 145 μM (Δ); aps-D1·D3, 162 μM (▲); ps-D5·D6, 150 μM (□), and aps-D5·D7, 135 μM (■).

mation of the helix–coil transition of each molecule. The release of counterions per mole of DNA duplex, ΔN_{Na^+}, that accompanies the helix–coil transition of each oligomer duplex was calculated using the following equation:[9]

$$dT_m/d \log [Na^+] = -0.9(2.303RT_m^2/\Delta H°_{cal})\Delta n_{Na^+} \quad (1)$$

The values of the slopes, $dT_m/d \log [Na^+]$, are obtained from plots of the T_m vs log [Na^+] at constant total strand concentration; the negative sign is to indicate a release of counterions; the value of 0.9 is a correction factor that corresponds to converting mean ionic activities to concentrations; R is the gas constant in cal/(K·mol); and $\Delta H°_{cal}$ (in cal/mol of duplex) is the standard duplex dissociation enthalpy, which is measured directly with differential scanning calorimetry. The counterion release obtained in this way corresponds to the thermodynamic ion release of the melting of one cooperative unit;[9] in two-state transitions this cooperative unit is equal to the dissociation of the entire duplex. These Δn_{Na^+} values in moles of sodium ions released per duplex can be normalized per phosphate by taking into account the total number of phosphates in the strands.

Results and Discussion

Calorimetric Transitions of Duplexes. We measured excess heat capacities as a function of temperature for all four duplexes (Figure 2). These curves show the presence of single transitions for all four duplexes. Integration of the area under these curves allows for the calculation of model-independent enthalpies, ΔH_{cal}.[13]

The enthalpies for the disruption of each duplex were endothermic with no differences in heat capacities. The values are in excellent agreement with the van't Hoff enthalpies obtained from shape analysis[13] of the heat capacity curves (Table I). The $\Delta H_{vH}/\Delta H_{cal}$ ratios are in the range 0.97–1.06, indicating that all duplexes melt in an all-or-none fashion with no intermediates.[13]

Our calorimetric enthalpies for the antiparallel duplexes are 56 kcal·mol^{-1} (aps-D1·D3) and 25 kcal·mol^{-1} (aps-D5·D7) lower than the enthalpy values predicted according to their nearest-neighbor composition.[14] The formation of partially paired intermolecular and intramolecular duplexes can be ruled out because the melting curves of the single strands (data not shown) displayed only a small percentage of single-strand stacking that completely disappeared at room temperature. Our determinations were performed in 0.1 M NaCl, as opposed to the 1 M NaCl used to estimate the nearest-neighbor parameters.[14] However, we found that the transition enthalpy was independent of salt concentration. That is, in 1 M NaCl we obtained ΔH_{cal} = −149 kcal·mol^{-1} and ΔH_{vH} = −144 kcal·mol^{-1} for aps-D1·D3, compared to the values of −151 and −150 kcal·mol^{-1}, respectively, in 0.1 M NaCl (Table I). The observed difference from the predicted ΔH_{cal} value could have other reasons: (1) The duplexes may have frayed ends, a phenomenon that is known to occur with terminal A·T base pairs.[12,15,16] In the calorimetric melting curve any fraying base pairs in the initial state will not contribute to the overall transition heats and thus will reduce the observed enthalpies. If one assumes that the extent of fraying in these duplexes is up to three AA/TT base pairs (or two base-pair stacks) at each end,[15,16] then this could amount to a reduction of ~36 kcal·mol^{-1}/duplex. (2) Both duplexes (particularly aps-D1·D3) contain runs of adenine that may adopt a conformation different from the standard B-DNA form and possibly have a lowered transition enthalpy. (3) Deviations from a 1:1 mixing ratio of strands would also lead to an apparent lower enthalpy; e.g., if one of the strands had been at a 10% higher

(14) Breslauer, K. J.; Frank, R.; Blocker, H.; Marky, L. A. *Proc. Natl. Acad. Sci. U.S.A.* **1986**, *83*, 3746.

(15) Otting, G. G.; Grutter, R.; Leupin, W.; Minganti, C.; Ganesh, K. N.; Sproat, B. S.; Gait, M. J.; Wuthrich, K. *Eur. J. Biochem.* **1987**, *166*, 215.

(16) Celda, B.; Widmer, H.; Leupin, W.; Chazin, W. J.; Denny, W. A.; Wuthrich, K. *Biochemistry* **1989**, *28*, 1462.

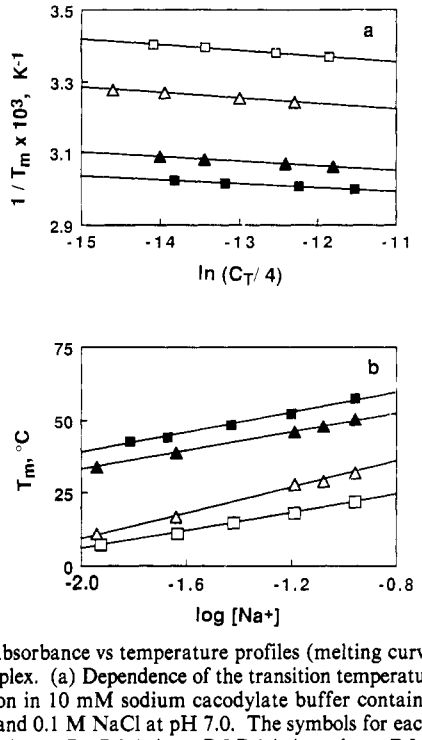

Figure 3. Absorbance vs temperature profiles (melting curves) for each oligomer duplex. (a) Dependence of the transition temperature on strand concentration in 10 mM sodium cacodylate buffer containing 0.1 mM Na_2EDTA and 0.1 M NaCl at pH 7.0. The symbols for each duplex are ps-D1·D2 (△), aps-D1·D3 (▲), ps-D5·D6 (□), and aps-D5·D7 (■). (b) Salt dependence of the transition temperature for the dissociation of each duplex; symbols as in panel a.

concentration, the measured enthalpy would have been reduced by 5%.

To confirm the two-state melting behavior of these duplexes, we monitored the temperature dependence of the UV absorbance as a second experimental observable for the measurement of model-dependent transition enthalpies. Such determinations have been reported previously for the same molecules.[4-8] From shape analysis of these curves, we can extract both the T_m and the transition enthalpy, ΔH_{shape}.[13] The slopes of $(1/T_m)$ vs $(\ln C_T/4)$ plots (Figure 3a) provide a more accurate spectroscopic determination of ΔH_{vH}.[13] The resulting model-dependent enthalpies are also given in Table I and are in good agreement with the calorimetric enthalpies, confirming the two-state melting behavior of all duplexes.

From the point of view of statistical mechanical theory of thermal transitions, the two-state melting behavior of the duplexes studied here is surprising.[17] That is, a finite contribution of partly unpaired intermediates would be expected. Unfortunately, direct comparison with literature data cannot be made because calorimetric studies of oligonucleotides as a function of chain length or with lengths comparable to the duplexes of this work have not been performed; the longest reported linear DNA duplexes with a two-state melting behavior are $d(GCGAATTCGC)_2$, $d(GAAGATCTTC)_2$, and $d(ATATATATAT)_2$.[14]

Standard Thermodynamic Profiles. The overall destabilization of 17 °C and 34 °C of the ps duplexes relative to the aps duplexes with identical sequences corresponds to $\Delta\Delta G°$ values of 11 and 18 kcal·mol^{-1} for the two pairs of duplexes (see Table I). The nature of this destabilization is purely enthalpic and probably corresponds to the loss of favorable hydrogen-bonding and base-stacking interactions as well as to changes in the degree of hydration. Furthermore, the substitution of four dA·dT base pairs of ps-D1·D2 for four dG·dC base pairs in the ps-D5·D6 duplex results in a destabilization of 11.9 °C, which is entropically driven. The same type of substitution in the aps duplexes results in a stabilization of 4.9 °C, which is enthalpically driven.

Counterion Binding to Parallel-Stranded DNA. Figure 3b shows the effect of counterions on the helix–coil transition in these duplexes. These curves indicate the shift of the helix–coil equilibria toward the helical state with increasing salt concentration. The slopes of these lines range from 16.9 to 21.8 °C and correspond, according to eq 1, to Δn_{Na^+} values ranging from 0.11–0.14 mol of Na^+/mol of phosphate. Since the single strands are similar in sequence, we conclude as in previous studies[4-8] that the ps duplexes and aps duplexes have similar charge densities.

Acknowledgment. This work was supported by Grant GM-42223 (L.A.M.) from the National Institutes of Health.

(17) D. Porschke, In *Molecular Biology, Biochemistry and Biophysics*; Pecht, I., Rigler, R., Eds.; Springer-Verlag: Berlin, 1977; Vol. 24, pp 191–218.

Understanding Enzyme-Catalyzed Proton Abstraction from Carbon Acids: Details of Stepwise Mechanisms for β-Elimination Reactions

John A. Gerlt* and Paul G. Gassman*

Contribution from the Department of Chemistry and Biochemistry, University of Maryland, College Park, Maryland 20742, and Department of Chemistry, University of Minnesota, Minneapolis, Minnesota 55455. *Received November 27, 1991*

Abstract: The observed rates of enzyme-catalyzed abstraction of a proton from a carbon adjacent to a carbonyl/carboxylic acid group (α-proton of a carbon acid) require that the pK_a of the α-proton be decreased such that it is equal to (±2–3 pK_a units) or less than that of the protonated active site basic catalyst. This can be accomplished by concerted general acid–general base catalysis: Gerlt, J. A.; Kozarich, J. W.; Kenyon, G. L.; Gassman, P. G. *J. Am. Chem. Soc.* **1991**, *113*, 9667. Analysis of various enzyme-catalyzed β-elimination reactions using this principle leads to the prediction that these reactions are likely to proceed via stepwise mechanisms which involve initial concerted general acid–general base catalyzed formation of an enol intermediate followed by elimination of the β-substituent. The second step is a vinylogous E2 reaction (1,4-elimination). Thus, these enzymes are not expected to catalyze "simple" E1cb reactions as has often been proposed. The involvement of concerted general acid–general base catalysis in reducing the pK_as of carbon acids may provide insight into the observed stereochemical courses of certain enzyme-catalyzed β-elimination reactions.

Introduction

The rapid rates of enzyme-catalyzed abstraction of a proton from a carbon adjacent to a carbonyl/carboxylic acid group (α-proton of a carbon acid) have long been puzzling, given the large difference between the pK_as of the substrate carbon acid in solution and the active site base:[1] in solution, the pK_as values of the

0002-7863/92/1514-5928$03.00/0